

February 3, 1999

*IN-91
021568*

A Final Report (Summary of Research) for Project No. 15-1668

NASA Grant Number NAG5-6767 (2/1/1998-1/31/1999)

High-Resolution Spectroscopy of Auroras on Jupiter and Saturn / Earth Dayglow

Prepared by:

**G. Randall Gladstone
Southwest Research Institute
6220 Culebra Road
San Antonio, TX 78238-5166**

**ph: 210-522-3581
fax: 210-543-0052
e-mail: randy@whistler.space.swri.edu**

Overview

The purpose of the grant to SwRI was to allow Dr. Gladstone to:

- Reduce and analyze ORFEUS-II observations of Jupiter (200s) and Saturn (1200s)
- Reduce and analyze selected ORFEUS-II Earth FUV airglow data.
- Modify existing scripts for simulating Earth FUV airglow emissions to model a subset of the ORFEUS-II data.

The rest of this report describes the results obtained in each of these areas.

Data Reduction and Analysis

The ORFEUS (Orbiting and Retrievable Far and Extreme Ultraviolet Spectrometers) telescope contains a normal incidence parabolic primary mirror 1 m in diameter. The Berkeley spectrograph covers the 39–122 nm band in 4 channels (A, B, C, and D) with a spectral resolution of $\sim \lambda/3000$ for point sources. Most science observations were performed with the 26" diameter aperture, for which the diffuse source resolution is about $\lambda/1000$. A second aperture, $\sim 30''$ in diameter and off-axis by $2.4'$, was used to obtain airglow spectra. The effective area varies with wavelength but is typically $\sim 6\text{--}9\text{ cm}^2$.

As expected, the extremely limited amount of Jupiter and Saturn data acquired by ORFEUS-II was insufficient to yield any useful scientific results. The Jupiter observation was so close to the Sun that the scattered background made tracking difficult, and only 200 s of data were obtained. Although Saturn was in much better position, after 1200 s of data were gathered it was determined to be too faint for continued observations.

In consultation with Dr. Mark Hurwitz (PI) and Dr. Van Dixon of the Berkeley Spectrometer team, we selected a set of D-channel airglow-aperture spectra made during 11 orbits from Nov. 21 to Dec. 31, 1996 (during target-aperture observations of the Seyfert 1 galaxy NGC4151), for our Earth airglow study. During the observations, strong airglow emissions were recorded for the He I 58.4 nm, O II 83.4 nm, O I 98.9 nm, HI 102.5 nm, NI 113.4 nm, and NI 120.0 nm features. The relevant observing parameters are presented in Table 1. Orbits #4 and #9 were chosen for detailed model simulation, since they occur during extremes in F10.7 and Ap for the data set.

Table 1. ORFEUS-II Airglow Observations

Orbit #	Date	Exp. Start	Exp. End	F10.7	Ap
1	11/21/96	12:51:29	13:08:09	72.6	2
2	11/22/96	16:17:46	16:37:06	80.6	5
3	11/23/96	18:02:00	18:42:11	88.7	6
4	11/26/96	13:11:59	13:44:41	100.8	12
5	11/28/96	20:05:08	20:38:24	95.4	5
6	11/29/96	21:49:06	22:23:06	88.5	6
7	11/30/96	04:12:00	04:34:00	85.1	2
8	11/30/96	05:38:00	05:56:00	85.1	2
9	11/30/96	19:21:53	19:54:23	85.1	0
10	12/2/96	06:40:05	06:58:32	75.7	3
11	12/3/96	17:46:50	18:02:59	70.7	7

Model Simulations

The position, zenith look angle, and solar zenith angle all vary considerably during the exposures, making analysis of the airglow data challenging [cf. Fig. 1]. To simulate the observed airglow emissions, we used the MSISE-90 atmosphere model, and our own photoelectron production/transport and radiative transfer codes. At each of 66 positions for each orbit the above models were run to generate radiances expected for the ORFEUS-II observing geometry for each likely source of the observed emission features. The average over each orbit of these runs were then compared with the ORFEUS-II data.

The O I 98.9 nm dayglow feature [cf. Fig. 2] is a sextuplet that is entirely excited by photoelectron impact, but is sometimes hard to simulate since it has a rather poorly-known branching ratio from the excited state (assumed to be 0.0002 here). The H I 102.6 nm feature [cf. Fig. 3] is primarily due to resonance scattering of the bright solar Ly β line, but with the added complication of a nearly coincident O I 102.7 nm sextuplet, which is excited both by photoelectron impact and by accidental resonance scattering of the solar Ly β line. Strong branching from the excited state prevents the O I 102.7 nm emission from becoming very bright. Modeling of the N I 120.0 nm feature [cf. Fig. 4] has been a problem for some time. However, thanks to recent N I 120.0 nm fluorescence cross sections for photodissociated and excited N₂, the problem seems to be solved—photodissociation and excitation of N₂ and electron impact excitation of N appear to contribute roughly equally to the observed emission.

The ORFEUS data are extremely well-calibrated (to an absolute level of 5–10%) through the

use of white-dwarf observations. Once calibration of the other spectrograph channels is complete, fitting the many emission features simultaneously will provide us with strong constraints on the input model atmospheres, solar EUV flux, cross sections, etc., required for our models. These model improvements can then be applied to existing (e.g., POLAR) and upcoming (e.g., TIMED, IMAGE) space physics missions that have or will acquire data of similar nature.

Publication of Results

The results remain to be written up for publication in the *Journal of Geophysical Research*. A presentation of the results was made at the fall 1998 meeting of the American Geophysical Union, as referenced below.

Gladstone, G. R., R. Link, W. Van Dixon, and M. Hurwitz, High spectral resolution observations of EUV airglow emissions from ORFEUS-II, Fall Annual Meeting, American Geophysical Union, San Francisco, 1998.

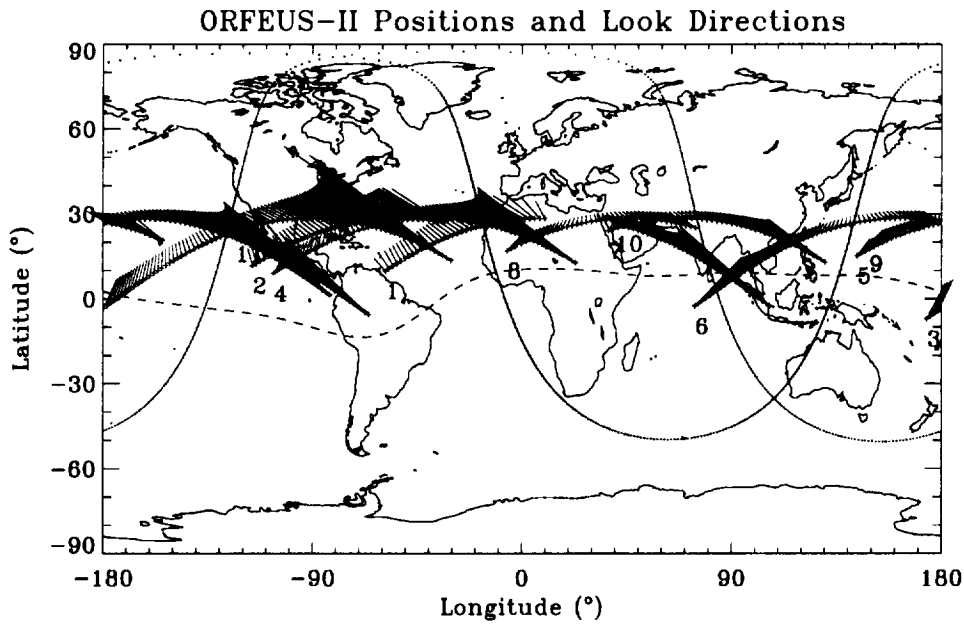


Fig. 1. Location of the ORFEUS-SPAS experiment in latitude and longitude during the NGC4151 exposures. Each of the 11 orbits is labeled near the start (western end) of each exposure. The extended lines from each location show the azimuth of the look direction toward the astronomical target at that instant. The end of each line corresponds to the point where the instrument line-of-sight crosses an altitude of 2000 km, which is the height used for the upper boundary of the model airglow simulations. Orbits #4 and #9, for which model simulations were performed, are shown in red and blue, respectively, along with the shadow boundary for an altitude of 350 km at each orbit's midpoint.

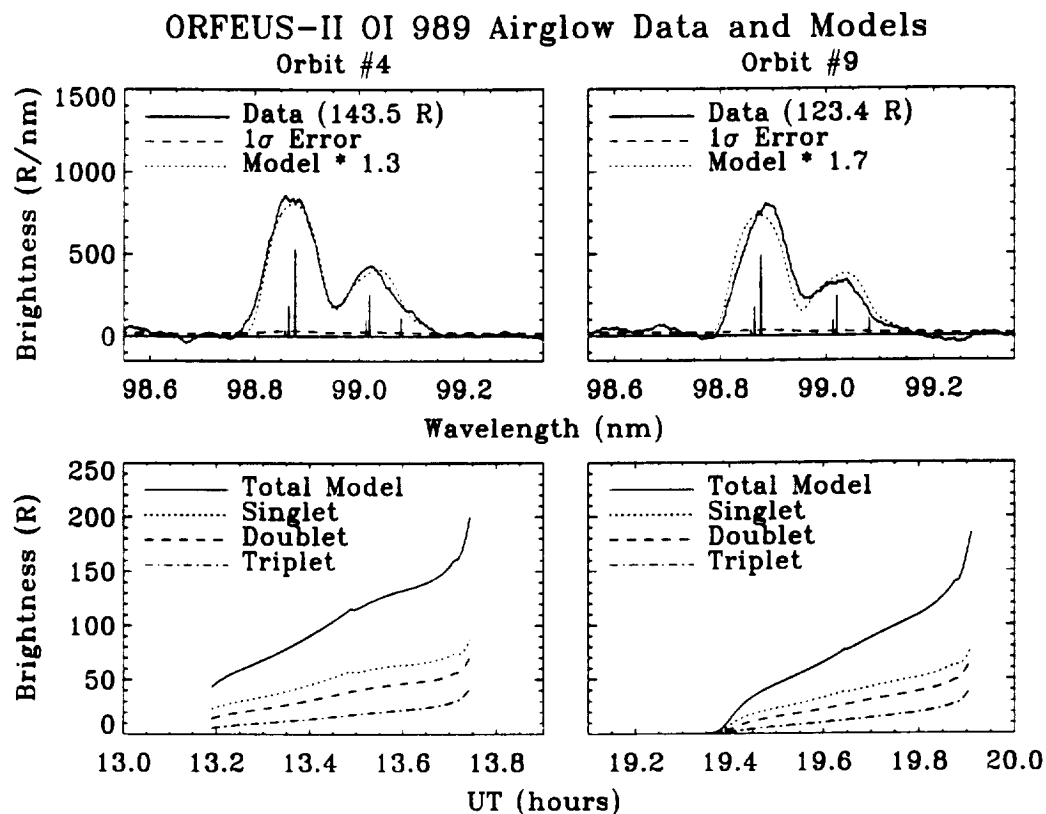


Fig. 2. Upper Panels: High-resolution comparison of ORFEUS-II spectra of the O I 98.9 nm airglow from orbits #4 and #9 with scaled model simulations. The dotted lines show the model results smoothed by the instrument function, while the narrow-line features are the actual model spectra. **Lower Panels:** Model (unscaled) brightness variation over the course of each orbit. The total O I 98.9 nm intensity is shown, along with a breakdown by multiplet component. The O I 98.9 nm feature is entirely excited by photoelectron impact on atomic oxygen.

ORFEUS-II HI 1026 & OI 1027 Airglow Data and Models

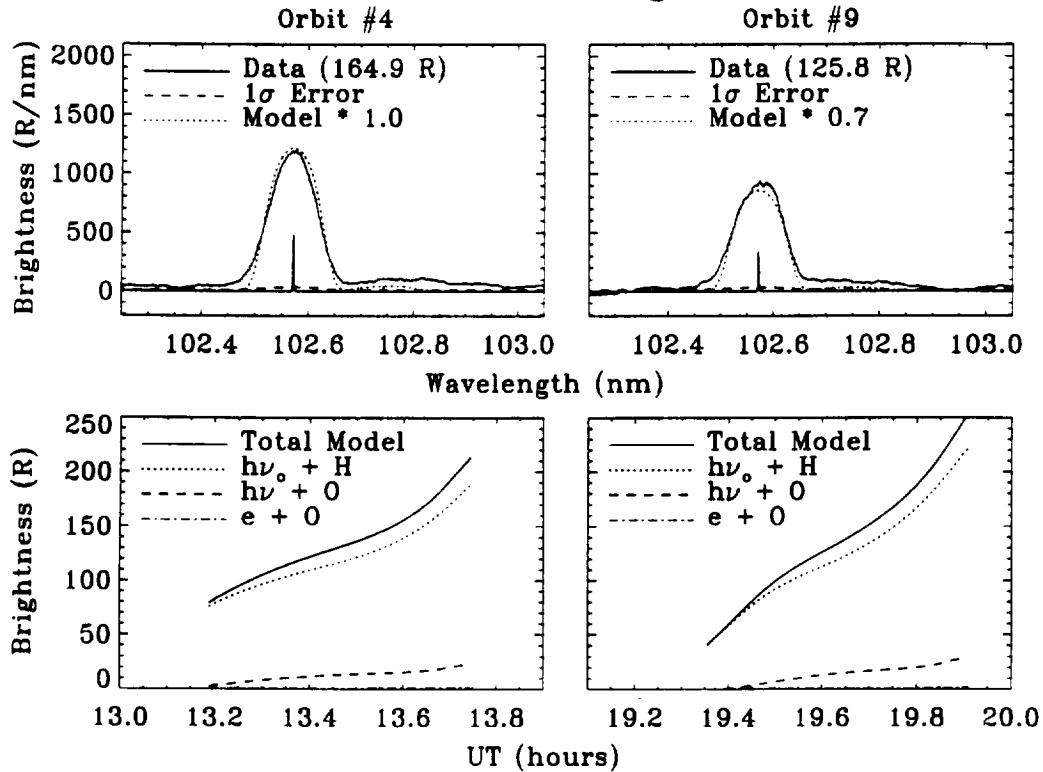


Fig. 3. Upper Panels: High-resolution comparison of ORFEUS-II spectra of the HI 102.6 nm and OI 102.7 airglow from orbits #4 and #9 with scaled model simulations. The dotted lines show the model results smoothed by the instrument function, while the narrow-line features are the actual model spectra. **Lower Panels:** Model (unscaled) brightness variation over the course of each orbit. The total HI 102.6 nm plus OI 102.7 nm intensity is shown, along with a breakdown by the three main sources. The HI 102.6 nm feature is entirely due to resonantly scattered solar Ly β , while the much weaker OI 102.7 nm feature is primarily due to accidental resonance scattering of the same solar Ly β , with a minor source due to electron impact on atomic oxygen.

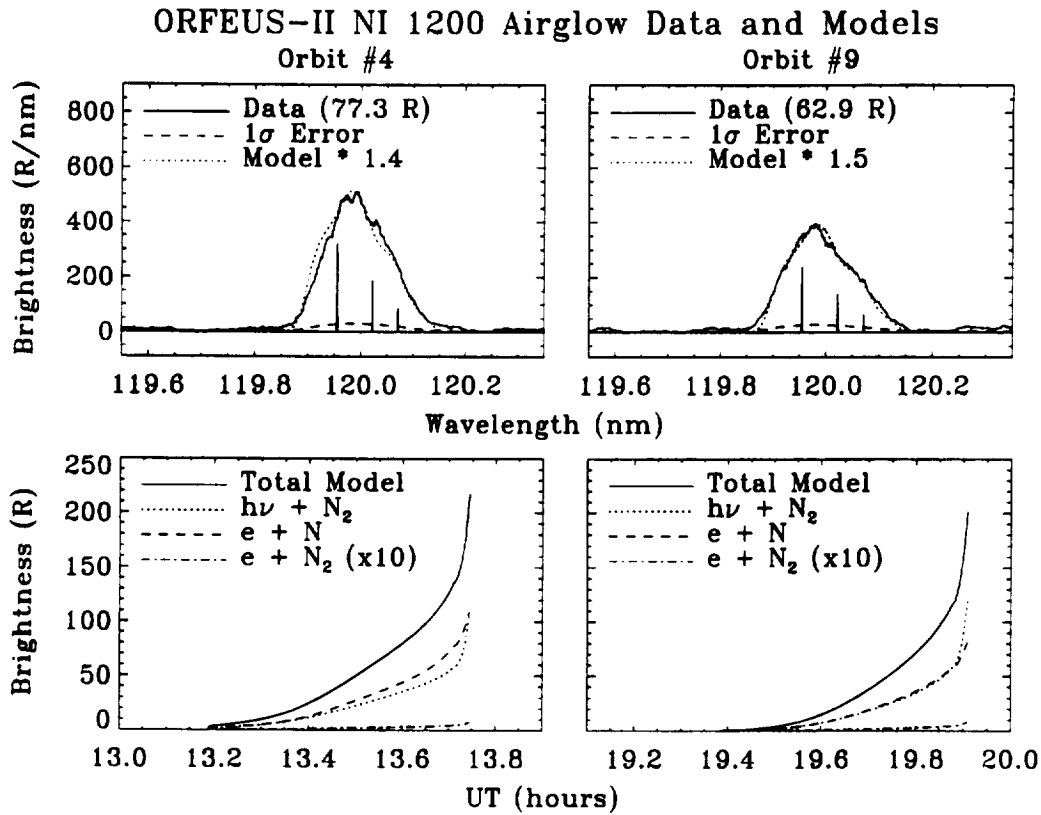


Fig. 4. Upper Panels: High-resolution comparison of ORFEUS-II spectra of the NI 120.0 nm airglow from orbits #4 and #9 with scaled model simulations. The dotted lines show the model results smoothed by the instrument function, while the narrow-line features are the actual model spectra. **Lower Panels:** Model (unscaled) brightness variation over the course of each orbit. The total NI 120.0 nm intensity is shown, along with a breakdown by the three main sources. The NI 120.0 nm feature is primarily due to a combination of photodissociation and excitation of N_2 and electron impact on atomic nitrogen, with a minor source due to electron impact dissociation and excitation of N_2 .